Electronic Supplementary Material (ESI) for Dalton Transactions.

Fe-N_4 engineering of S,N co-doped hierarchical porous carbon-based electrocatalysts for enhanced oxygen reduction in Zn-air battery

Jingxia Gao [a], Sa Liu *, [a], Ping Zhu [a], Xinsheng Zhao *, [b], Guoxiang Wang [c]

[a] School of Chemistry and Materials Science, Jiangsu Key Laboratory of Green Synthetic for Functional Materials, Jiangsu Normal University, Xuzhou 221116, People's Republic of China

[b] School of Physics and Electronic Engineering, Jiangsu Normal University, Xuzhou 221116, People's Republic of China

[c] School of Light Industry & Chemical Engineering, Dalian Polytechnic University, Dalian 116034, People's Republic of China

Experimental section

Characterizations: Scanning electron microscopy (SEM) was obtained on HITACHI S-8010. Transmission electron microscopy (TEM), high-resolution TEM (HRTEM) and scanning transmission electron microscope (STEM) were recorded by FEI Tecnai G2 F20. X-ray diffraction (XRD) was carried out on a Bruker AXS D8ADVANCE diffractometer. X-ray photoelectron spectroscopy (XPS) was used to evaluate the surface element on ESCALAB 250Xi. ^{57}Fe Mössbauer spectrum was obtained with a ^{57}Co:Rh source on a Topologic 500A spectrometer driving with a proportional counter at room temperature. Raman spectra were recorded on LabRAM HR800 equipment. The pores characterizations and surface area were obtained from nitrogen absorption/desorption isotherms measured on Quantachrome Autosorb IQ2-VP, and the pore size distribution were calculated by density function theory (DFT) method. Thermogravimetric analysis (TGA) was performed on a TA Q50 instrument with a heating rate of 5 ^{o}C min^{-1} and air atmosphere.

Electrochemical characterizations: Electrocatalytic performance was measured by a three-electrode system on electrochemical workstation (CHI 700D). Platinum wire and Ag/AgCl (in 3.5 M KCl) electrode were used as the counter electrode and reference electrode, respectively. 5 mg of as-prepared samples was dispersed in 0.6 ml of ethanol and 50 μL of Nafion (5 wt.%). Then 6.5 μL of the catalyst ink was dropped on 4 mm of rotating disk electrode (RDE) or rotating ring-disk electrode (RRDE) to obtain the working electrode. For comparison, the working electrode with

commercial Pt/C (20 wt.%) at a loading 100 μg cm^{-2} (20 μg_{Pt} cm^{-2}) was also prepared as the above similar method.

Steady cyclic voltammetry (CV) was recorded between 0-1.2 V (vs. RHE) at a sweep rate of 50 mV s^{-1} in N_2 and O_2-saturated 0.1 M KOH. Linear sweep voltammetry (LSV) was collected at a scanning rate of 10 mV s^{-1} and different electrode rotating rate (100-2500 rpm) in O_2-saturated 0.1 M KOH.

The Koutecky-Levich (K-L) plots were calculated by the following equations,

$$\frac{1}{j}=\frac{1}{j_k}+\frac{1}{j_L}=\frac{1}{j_k}+\frac{1}{B}\omega^{-1/2} \quad (1)$$

$$B=0.2nFC_0D_0^{2/3}\vartheta^{-1/6} \quad (2)$$

Here, j_K is the kinetic current density (mA cm^{-2}), j_L is the limiting diffusion current density (mA cm^{-2}), n is the electron transfer number, F is the Faraday constant (96485 C mol^{-1}), C_0 (1.2×10^{-6} mol cm^{-2}) and D_0 (1.9×10^{-5} cm^2 s^{-1}) are the concentration and diffusion coefficient of O_2 in 0.1 M KOH, respectively. υ is the kinematic viscosity of 0.1 M KOH (0.01 cm^2 s^{-1}).

The H_2O_2 yield and the electron transfer number were measured on RRDE by the following equations,

$$H_2O_2(\%)=\frac{200I_R}{I_R+NI_D} \quad (3)$$

$$n=\frac{4NI_D}{I_R+NI_D} \quad (4)$$

Here, I_D is the measured disk current (mA), I_R is the measured ring current (mA) when 1.2 V was applied to the ring, N is the electrode collection efficiency (42.4%).

Chronoamperometric response at 0.7 V was measured in the O_2-saturated 0.1 M

KOH solution with or without 1 M methanol.

Accelerated durability tests (ADTs) were carried out by continuous CV cycling (10000 cycles) in O_2-saturated 0.1 M KOH at a scan rate of 200 mV s^{-1} between 0.6 and 1.2 V.

ZABs measurement: A clean zinc plate of 0.5 mm thickness was served as anode of a home-made ZAB. 6 M KOH and 6 M KOH+0.2 M zinc acetate were used as electrolyte for primary ZAB and rechargeable ZAB, respectively. The air electrode was prepared as follows: the above as-prepared catalysts ink was dropped on the gas-diffusion layer attacted with carbon paper of an effective area of 1 cm^2. The catalyst loading was 0.5 mg cm^{-2}. For comparison, the commercial Pt/C (20 wt.%)-loaded air electrode was also prepared with a same catalyst loading.

The solid-state ZAB was assembled by using FeSN-HPC loaded GDL (1 mg cm^{-2}) as air electrode, Zn plate as anode, and gel of polyvinyl alcohol (PVA)/KOH as the solid-state electrolyte. The gel electrolyte was prepared by a typical procedure as follows: 1.0 g of PVA was dissolved into 10 mL of H_2O at 95 ^oC, followed by adding 1 mL of 18.0 M KOH solution. Subsequently, the mixture was stirred at 95 ^oC for 30 min to obtain a uniform solution. Then the solution was poured into a culture dish, frozen at -20 ^oC for 12 h and thawed at room temperature. The process was repeated three times to get a uniform gel electrolyte.

The discharge polarization curve of ZAB was obtained on CHI 700D, and the charge-discharge cycling was recorded on LAND testing system.

Results

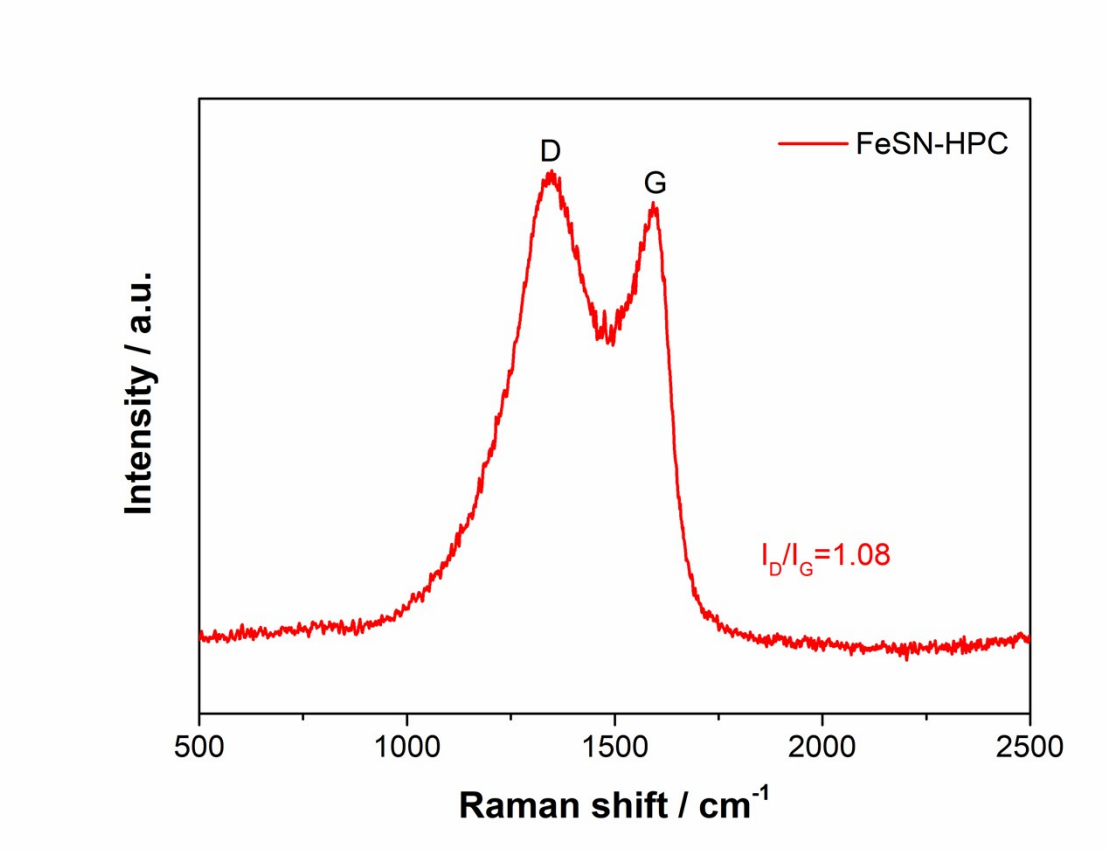

Fig. S1 Raman spectrum of FeSN-HPC.

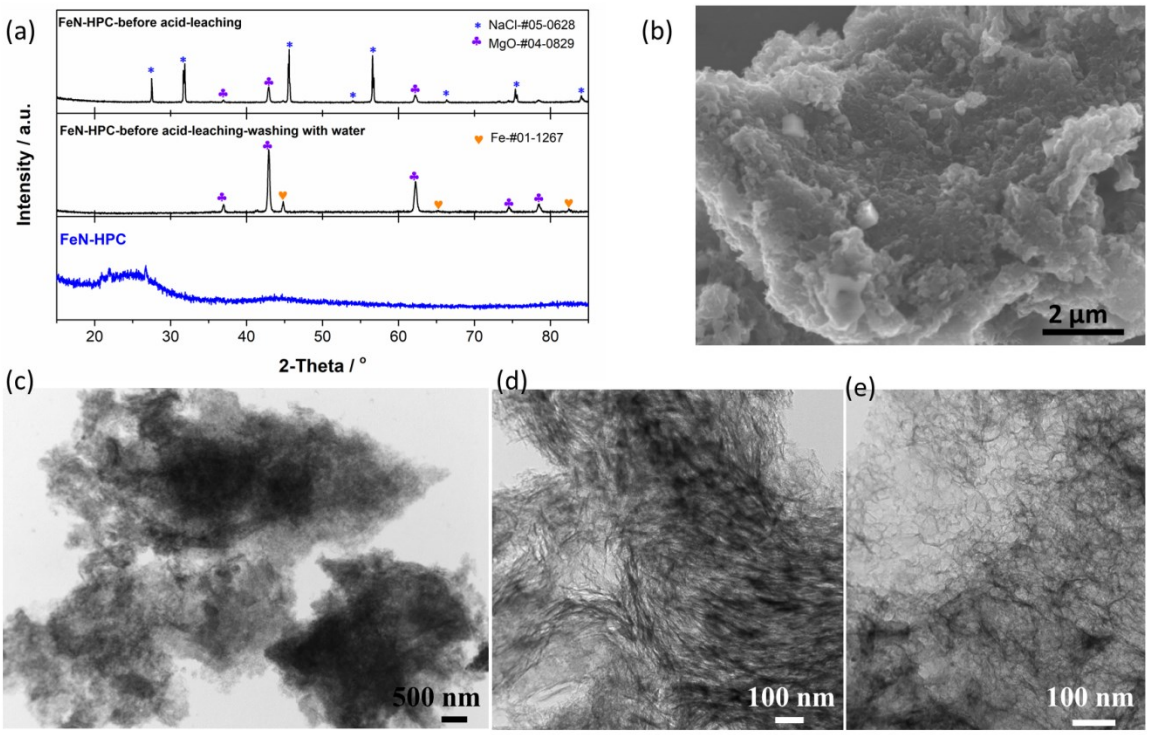

Fig. S2 (a) XRD patterns of FeN-HPC during the preparation process; (b) SEM and (c-e) TEM images of FeN-HPC.

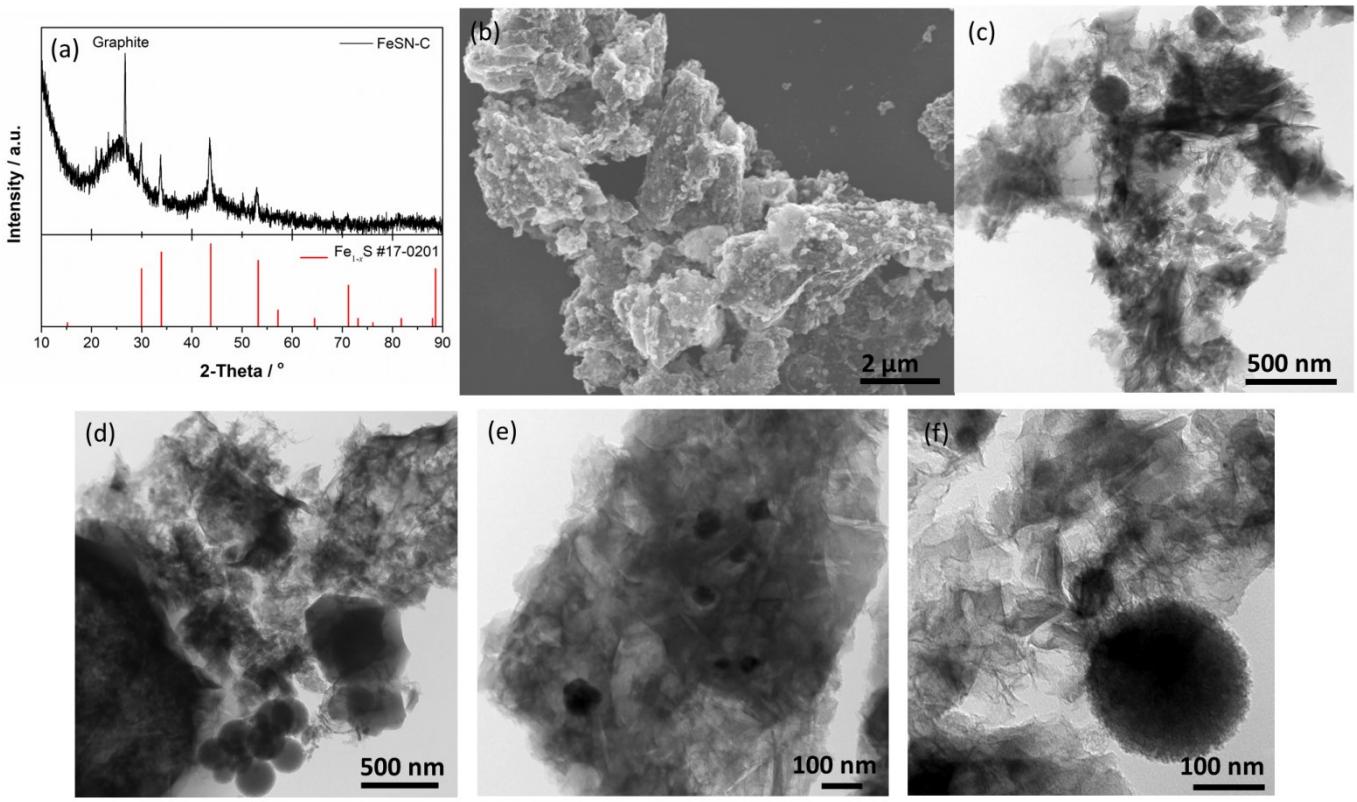

Fig. S3 (a) XRD pattern, (b) SEM and (c-f) TEM images of FeSN-C.

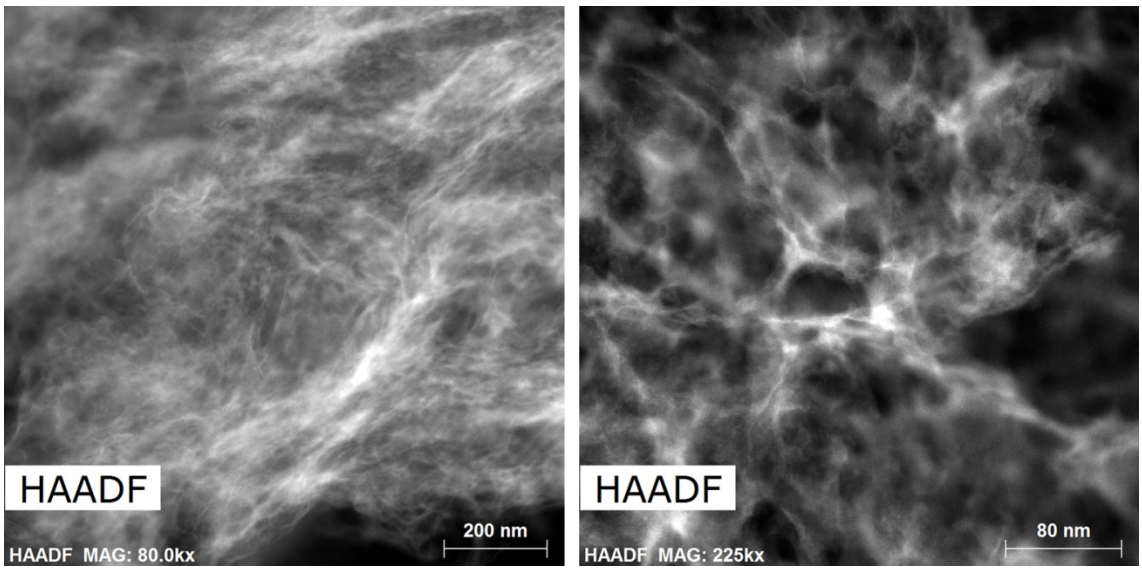

Fig. S4 HADDF-STEM images of FeSN-HPC.

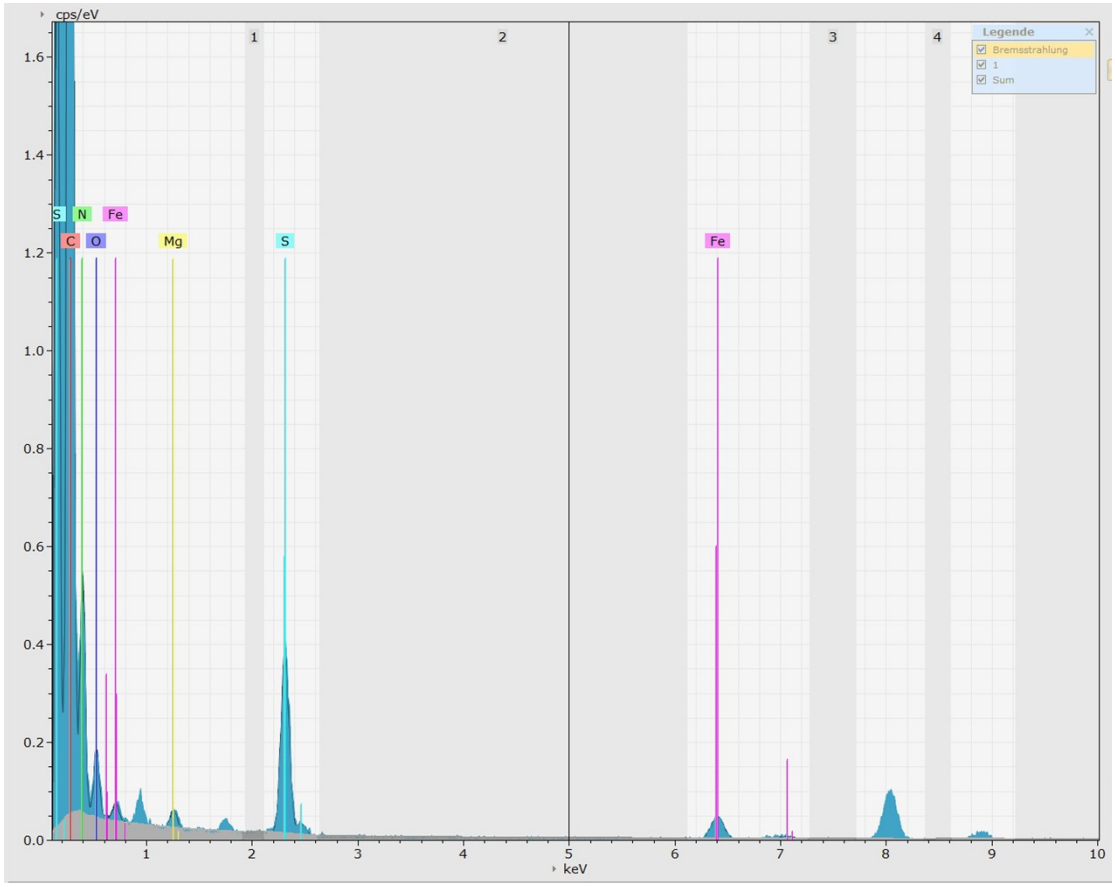

Fig. S5 EDS spectrum of the FeSN-HPC.

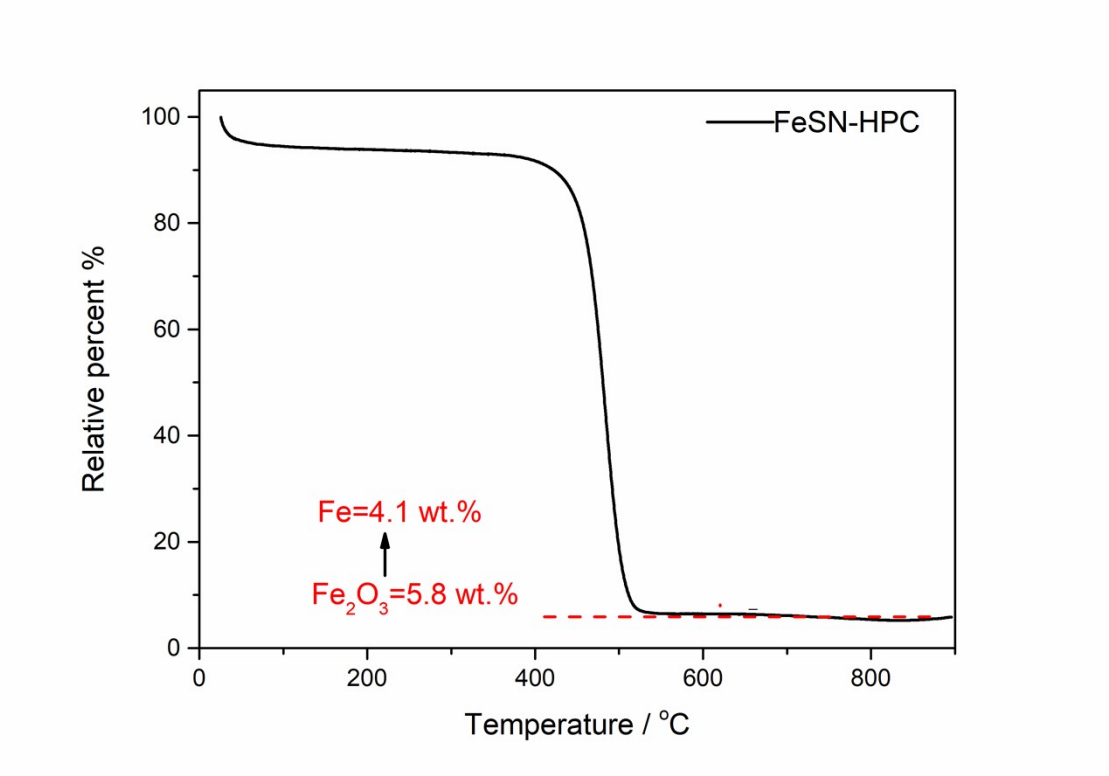

Fig. S6 TGA curve of FeSN-HPC under air atmosphere.

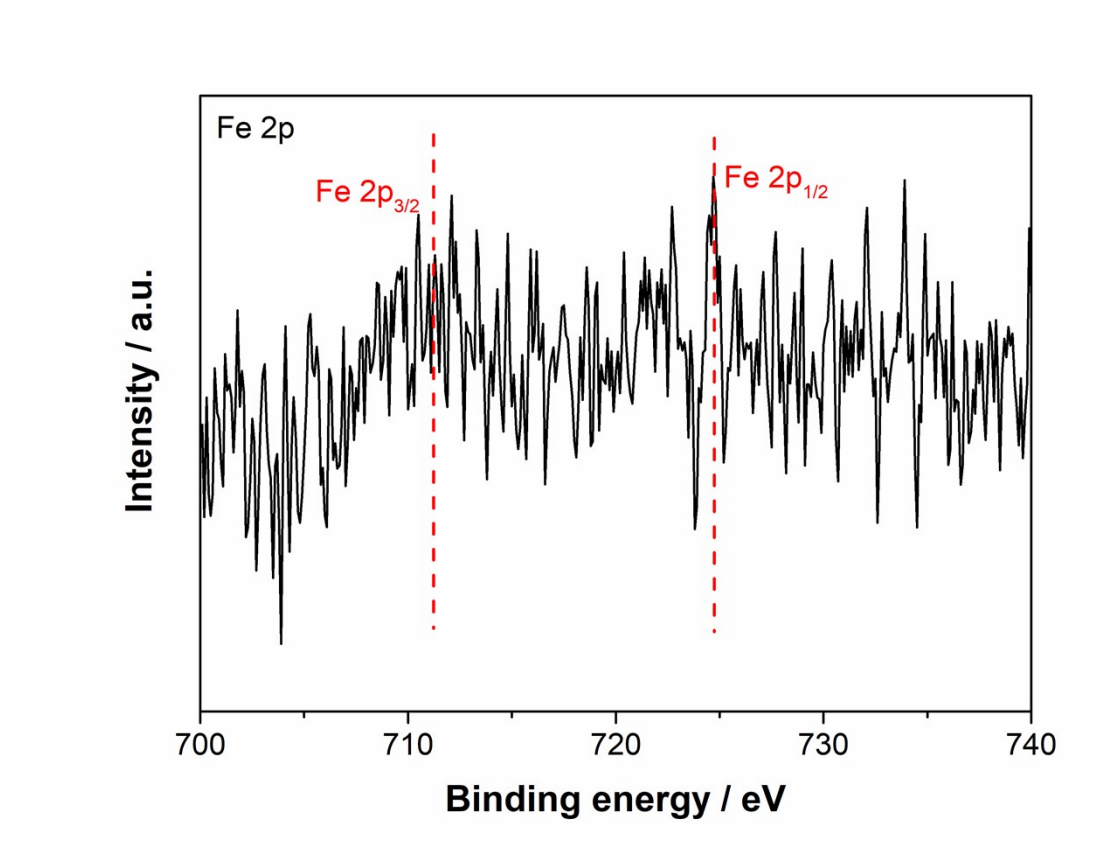

Fig. S7 The high resolution Fe 2p XPS spectra of as-prepared FeSN-HPC.

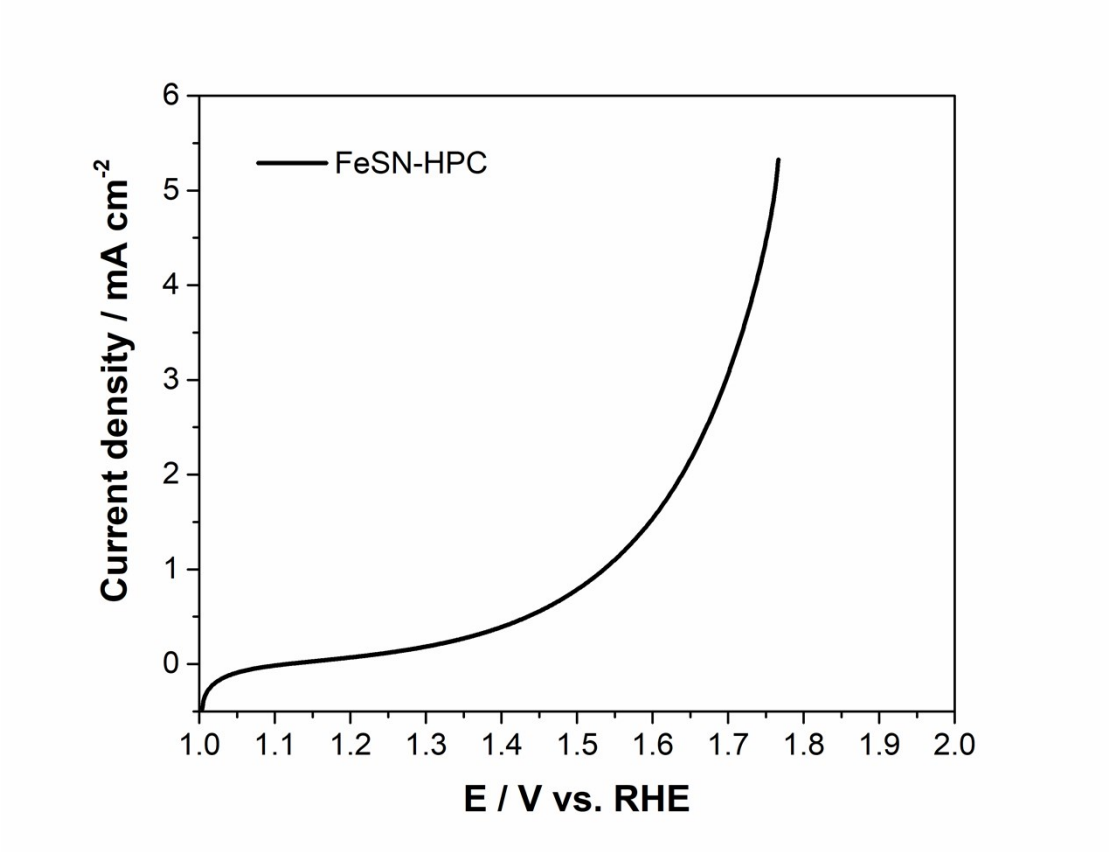

Fig. S8 OER polarization curves of FeSN-HPC in O_2-saturated 0.1 M KOH at a scanning rate of 10 mV s^{-1} and a electrode rotating rate of 1600 rpm.

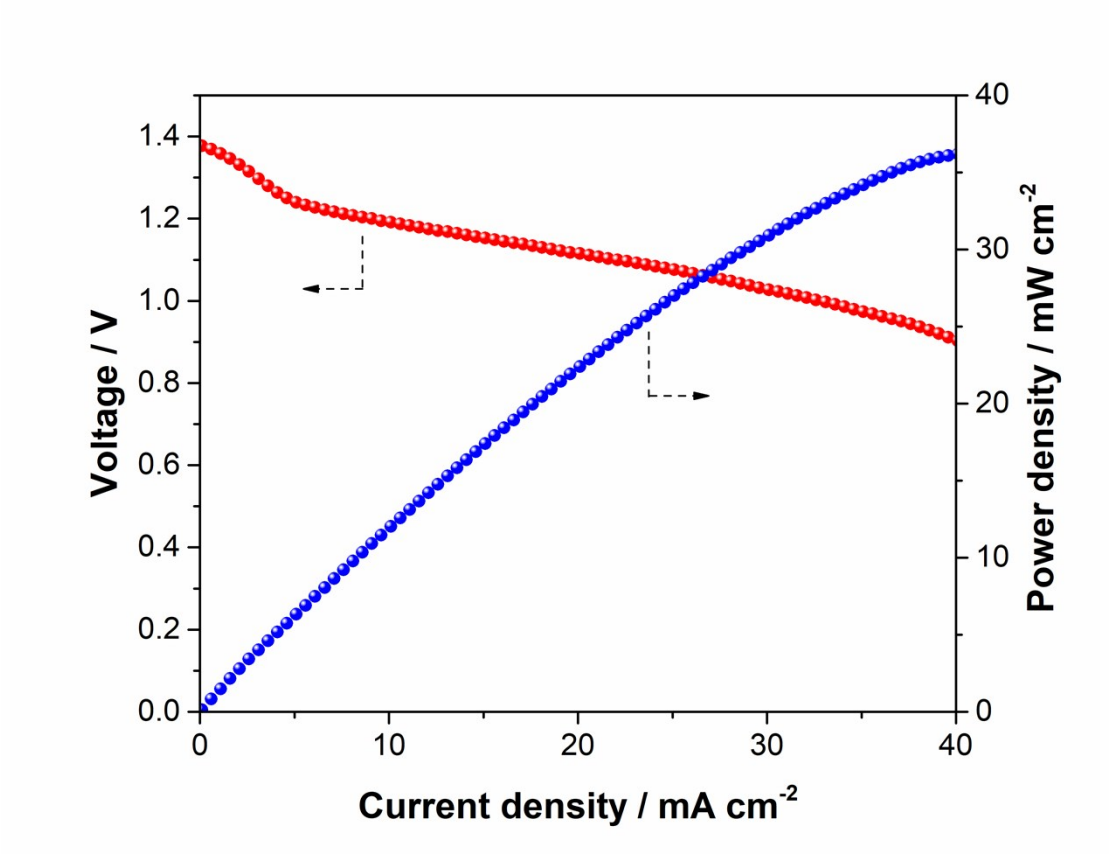

Fig. S9 The discharge polarization and power density curves of solid ZAB with FeSN-HPC-loading air electrode.

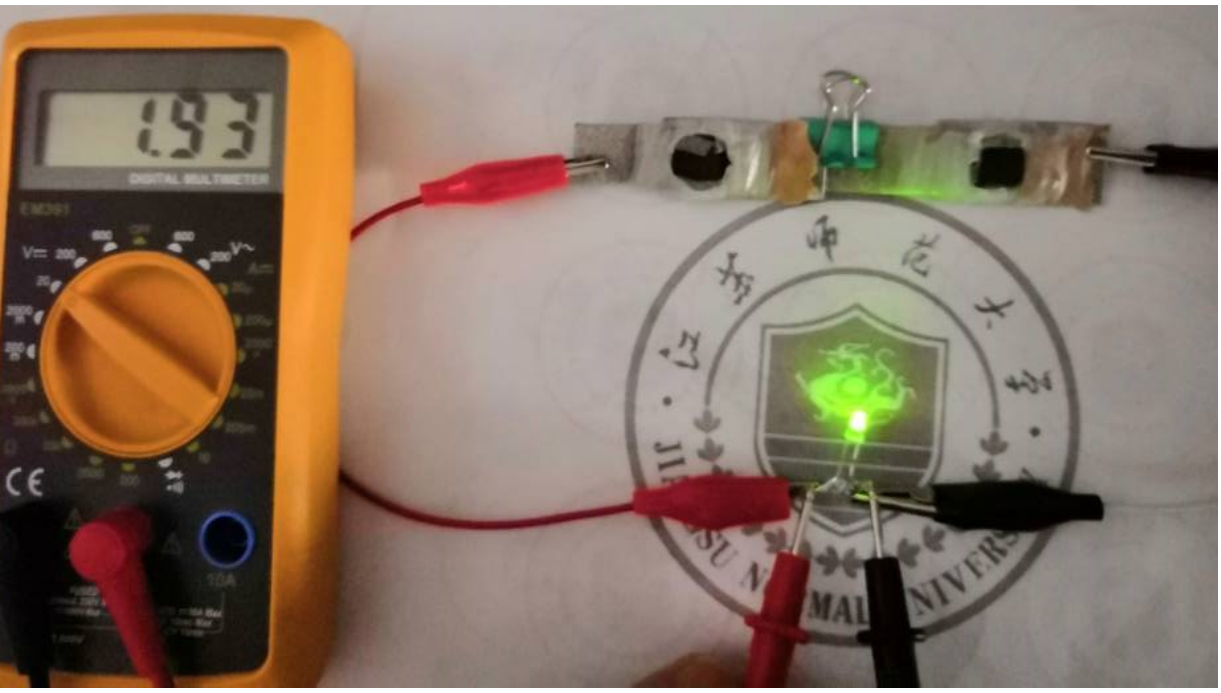

Fig. S10 A photograph of a light LED powered by two FeSN-HPC-catalyzed ZABs in series. A multimeter showed that the working power of the light LED was 1.93 V.

Table S1 ^{57}Fe Mössbauer parameters (δ_{iso}, Isomer Shift; ΔE_Q, Quadrupole Splitting; FWHM, Full Width at Half-Maximum) and assignment to iron species for different Mössbauer sites

	δ_{iso}/	ΔE_Q/	FWHM/	area %	Assignment
			mm s^{-1}		
D1	0.46	1.02	0.62	42.90	$Fe^{II}N_4$, LS[1, 2]
D2	0.23	3.50	0.67	12.70	$Fe^{II}N_4$, MS[1, 3, 4]
D3	1.18	3.53	0.65	10.60	$Fe^{II}N_4$, HS[1, 4]
D4	0.29	0.86	0.74	33.80	$Fe^{III}N_4$, HS[5]

δ_{iso}: isomeric shift; ΔE_Q: quadrupole splitting; FWHM: full width at half maximum.

Table S2. The electrochemical performance of different catalysts reported recently in O_2-saturated 0.1 M KOH.

Sample	E_{onset} / V	$E_{1/2}$ / V	*n*	Ref.
FeSN-HPC	0.96	0.86	3.89-4.00	This work
a-MnO_x/TiC	0.96	0.8	~4.0	[6]
Fe/Fe_3C@N-C-NaCl	0.970	0.869	>3.9	[7]
Ionogel-Fe-C-N	1.00	0.870	3.99	[8]
Co 16%-NCNT-T800	-	0.815	3.25	[9]
Fe@C-NG/NCNTs	0.93	0.84	3.9-4.0	[10]
Co@NCNT HMS	0.980	0.857	3.85	[11]
N-CNT-900-NH_3	1.02	0.88	3.88-4.00	[12]
Co/N-BCNTs	-	0.83	3.75	[13]
Co/CoP-HNC	0.94	0.83	4.0	[14]

co-doped np-graphene	0.987	0.845	3.9	[15]
Zn/CoN-C	1.004	0.861	4.0	[16]
P-T/rGO	0.94	0.79	3.48	[17]
$Fe_3C@B_{1.0}NPCFs$	0.968	0.832	~4.0	[18]
Fe-S,N-C	0.95	0.83	> 3.94	[19]
CoPNi-N/C	0.93	0.84	3.9	[20]

Reference

1. U. I. Kramm, J. Herranz, N. Larouche, T. M. Arruda, M. Lefevre, F. Jaouen, P. Bogdanoff, S. Fiechter, I. Abs-Wurmbach, S. Mukerjee and J. P. Dodelet, *Phys Chem Chem Phys*, 2012, **14**, 11673-11688.
2. Q. Jia, N. Ramaswamy, U. Tylus, K. Strickland, J. Li, A. Serov, K. Artyushkova, P. Atanassov, J. Anibal, C. Gumeci, S. C. Barton, M.-T. Sougrati, F. Jaouen, B. Halevi and S. Mukerjee, *Nano Energy*, 2016, **29**, 65-82.
3. U. I. Kramm, M. Lefevre, N. Larouche, D. Schmeisser and J. P. Dodelet, *J Am Chem Soc*, 2014, **136**, 978-985.
4. J. Wang, Z. Huang, W. Liu, C. Chang, H. Tang, Z. Li, W. Chen, C. Jia, T. Yao, S. Wei, Y. Wu and Y. Li, *J Am Chem Soc*, 2017, **139**, 17281-17284.
5. W. Liu, L. Zhang, X. Liu, X. Liu, X. Yang, S. Miao, W. Wang, A. Wang and T. Zhang, *J Am Chem Soc*, 2017, **139**, 10790-10798.
6. S. Song, W. Li, Y.-P. Deng, Y. Ruan, Y. Zhang, X. Qin and Z. Chen, *Nano Energy*, 2019, DOI: 10.1016/j.nanoen.2019.104208.
7. Y. Zhang, L.-B. Huang, W.-J. Jiang, X. Zhang, Y.-Y. Chen, Z. Wei, L.-J. Wan and J.-S. Hu, *J. Mater. Chem. A*, 2016, **4**, 7781-7787.
8. S. Liu, Z. Yang, M. Li, L. Liu, Y. Wang, W. Lv, Z. Qin, X. Zhao, P. Zhu and G. Wang, *Electrochimica Acta*, 2018, **265**, 221-231.
9. Y. Zhang, L. Lu, S. Zhang, Z. Lv, D. Yang, J. Liu, Y. Chen, X. Tian, H. Jin and W. Song, *Journal of Materials Chemistry A*, 2018, **6**, 5740-5745.
10. Q. Wang, Y. Lei, Z. Chen, N. Wu, Y. Wang, B. Wang and Y. Wang, *Journal of Materials Chemistry A*, 2018, **6**, 516-526.
11. Y. Li, J. Gao, F. Zhang, Q. Qian, Y. Liu and G. Zhang, *Journal of Materials Chemistry A*, 2018, **6**, 15523-15529
12. X. Zhu, Y. Zhu, C. Tian, T. Jin, X. Yang, X. Jin, C. Li, H. Wang, H. Liu and S. Dai, *Journal of Materials Chemistry A*, 2017, **5**, 4507-4512.
13. R. Wang, T. Yan, L. Han, G. Chen, H. Li, J. Zhang, L. Shi and D. Zhang, *Journal of Materials Chemistry A*, 2018, **6**, 5752-5761.

14. V. Di Noto, E. Negro, K. Vezzù, F. Bertasi and G. Nawn, *The Electrochemical Society Interface*, 2015, **24**, 59-64.
15. H. J. Qiu, P. Du, K. Hu, J. Gao, H. Li, P. Liu, T. Ina, K. Ohara, Y. Ito and M. Chen, *Adv Mater*, 2019, **31**, e1900843.
16. Z. Lu, B. Wang, Y. Hu, W. Liu, Y. Zhao, R. Yang, Z. Li, J. Luo, B. Chi, Z. Jiang, M. Li, S. Mu, S. Liao, J. Zhang and X. Sun, *Angew Chem Int Ed Engl*, 2019, **58**, 2622-2626.
17. X. Long, D. Li, B. Wang, Z. Jiang, W. Xu, B. Wang, D. Yang and Y. Xia, *Angew Chem Int Ed Engl*, 2019, **58**, 11369-11373.
18. T. Liu, M. Li, X. Bo and M. Zhou, *J Colloid Interface Sci*, 2019, **533**, 709-722.
19. S. Liu, L. liu, X. Chen, Z. Yang, M. Li, Y. Wang, W. Lv, P. Zhu, X. Zhao and G. Wang, *Electrocatalysis*, 2019, **10**, 72-81.
20. Z. Li, H. He, H. Cao, S. Sun, W. Diao, D. Gao, P. Lu, S. Zhang, Z. Guo, M. Li, R. Liu, D. Ren, C. Liu, Y. Zhang, Z. Yang, J. Jiang and G. Zhang, *Applied Catalysis B: Environmental*, 2019, **240**, 112-121.